Solution-Processable Field-Effect Transistor Using a Fluorene- and Selenophene-Based Copolymer as an Active Layer

Young Mi Kim,[†,#] Eunhee Lim,[†] In-Nam Kang,[‡] Byung-Jun Jung,[†] Jaemin Lee,[†] Bon Won Koo,[§] Lee-Mi Do,[⊥] and Hong-Ku Shim*[,†]

Department of Chemistry and School of Molecular Science (BK21), Korea Advanced Institute of Science and Technology, Daejeon 305-701, Korea, The Catholic University of Korea, Bucheon, Gyeonggi-do 420-743, Korea, Samsung Advanced Institute of Technology, Yongin, Gyeonggi-do 449-712, Korea, and Basic Research Laboratory, Electronics and Telecommunications Research Institute, Daejeon 305-350, Korea

Received March 13, 2006; Revised Manuscript Received April 15, 2006

ABSTRACT: We have synthesized a new p-type polymer, poly(9,9′-*n*-dioctylfluorene-*alt*-biselenophene) (F8Se2), via the palladium-catalyzed Suzuki coupling reaction. The number-average molecular weight (M_n) of F8Se2 was found to be 72 600. F8Se2 dissolves in common organic solvents such as chloroform and chlorobenzene. The PL emission peak of a film of F8Se2 is clearly red-shifted with respect to that of its sulfur analogue, poly(9,9′-*n*-dioctylfluorene-*alt*-bithiophene) (F8T2), due to the electron-donating properties of selenium and the strong interactions between the biselenophene moieties in neighboring copolymer chains. We confirmed that F8Se2 is a thermotropic liquid crystalline polymer with an aligned structure by carrying out DSC, PLM, and XRD measurements. The introduction of the selenophene moiety into the liquid-crystalline polymer system results in better field-effect transistor (FET) performance than that of F8T2. A solution-processed F8Se2 FET device with a bottom contact geometry was found to exhibit a hole mobility of 0.012 $cm^2/(V\ s)$ and a low threshold voltage of −4 V, which is the one of the highest solution-processable FET performances.

Introduction

Organic semiconductors have recently received significant attention because of their applications as active layers in organic electronic devices such as organic light-emitting diodes (OLEDs),[1−3] organic field-effect transistors (OFETs),[4−8] and photovoltaic devices.[9−12] Organic FETs can be used in low-cost memories, smart cards, and the driving circuits of large-area display devices.[13−15] To minimize manufacturing costs, the FET fabrication process should ideally include solution-based methods such as spin-coating, stamping, or ink-jet printing. The use of soluble polymeric semiconductors has made possible the development of active-matrix multipixel displays using solution-based technology.[16]

Most p-channel organic semiconductors fabricated so far have been based on thiophene-derived oligomers and polymers. A few other systems that rely on aromatic macrocyclics such as metallophthalocyanines or fused aromatic rings such as pentacene and tetracene have also been developed.[17,18] Most of these semiconductors have relatively low band gaps and high highest occupied molecular orbital (HOMO) levels. Therefore, they tend to be easily oxidized, which results in their degradation. To solve these problems, the design and synthesis of organic semiconductors with a high charge carrier mobility and good stability are desirable. With this aim in mind, FETs based on fluorene-based copolymers have recently been reported. Fluorene-based polymers have better stability than thiophene-based polymers because of their rigid structures and lower HOMO levels as well as good film-forming and hole-transporting properties.[19] Interest in these copolymers was sparked by research showing that enhanced charge carrier mobility could be achieved in poly(9,9′-*n*-dioctylfluorene-*alt*-bithiophene) (F8T2) by aligning the polymer chains in the liquid-crystalline (LC) phase.[20] We have also reported the FET behaviors of the fluorene-thieno[3,2-*b*]-thiophene-based conjugated copolymer (F8TT). In that study, the introduction of groups with high degrees of planarity and rigidity was found to result in polymers that are more crystalline and that offer better FET device performance.[21] LC copolymers based on fluorene are potential candidates for solution-processable OFET semiconductor materials, and further development of this class of polymers is still required.

Selenophene is a heavy homologue of the series of chalcogenophenes and exhibits chemical and physical properties that are similar to those of thiophene.[22] Although polyselenophenes and oligoselenophenes have been little studied so far due to their low solubility and the lack of suitable synthetic methods and reagents, the replacement of sulfur by selenium is an interesting approach to the search for highly conducting organic materials. Selenium-containing oligomers have been used in OFETs with the aim of changing the stacking of neighboring molecules. Otsubo et al. have reported the FET behaviors of the oligoselenophene and fused selenophhene compounds. In that study, the selenophene-containing oligomers were vacuum-deposited at elevated substrate temperature, and the resulting FET devices showed high hole mobilities of up to $10^{-1}-10^{-3}$ $cm^2/(V\ s)$, which are higher than those of the thiophene-containing oligomers.[23−25]

Our focus in this study was to examine whether the introduction of Se-containing moieties into the liquid-crystalline polymeric system improves charge carrier transport in OFET devices. In the present work, we introduced biselenophene units into a fluorene-based alternating copolymer. The resulting liquid-crystalline polymer, F8Se2, was found to provide a high FET

[†] Korea Advanced Institute of Science and Technology.
[‡] The Catholic University of Korea.
[§] Samsung Advanced Institute of Technology.
[⊥] Electronics and Telecommunications Research Institute.
[#] Current address: LG Philips LCD R&D center, Anyang, Gyeonggi-do 431-080, Korea.
* To whom correspondence should be addressed. E-mail: hkshim@kaist.ac.kr.

10.1021/ma060567l CCC: $33.50
Published on Web 05/19/2006

device performance with a hole mobility of up to 10^{-2} cm^2/(V s) because of strong interchain interactions. The general properties of this derivative, including its liquid-crystalline and optical properties, were investigated to identify the nature of the mesophase of the F8Se2 film.

Experimental Section

2,2-Biselenophene (1). Into a stirred solution of selenophene (5 g, 38.16 mmol) in dry ether (70 mL) at 0 °C under a nitrogen atmosphere was added a 2.5 N hexane solution of butyllithium (15.264 mL, 38.16 mmol) over a period of 10 min, and the mixture was stirred for 1 h at RT to produce 2-lithioselenophene. After copper(II) chloride (6.81 g, 50.18 mmol) was added portionwise to the mixture cooled to −70 °C, the mixture was stirred overnight at RT, diluted with ether (50 mL), and filtered. The solid was thoroughly washed with ether, and the filtrate and washings were combined and successively washed with water, 1 N hydrochloric acid, 5% sodium hydrogen carbonate aqueous solution, and finally water. After the solvent had been evaporated, the residue was purified with column chromatography and recrystallization in methanol to provide **1** as a yellow solid (0.8 g, 33%). ^{1}H NMR ($CDCl_3$, 400 MHz): δ (ppm) 7.21 (dd, 2H), 7.25 (d, 2H), 7.86 (d, 2H). ^{13}C NMR ($CDCl_3$, 400 MHz): δ (ppm) 126.7, 129.6, 130.2.

5,5-Dibromo-2,2-biselenophene (2). Into a stirred solution of biselenophene (**1**) (0.5 g, 1.92 mmol) in chloroform−acetic acid (1:1 v/v 20 mL), NBS (0.69 g, 3.84 mmol) was added portionwise, and the mixture was stirred at RT for 1 h and then at 50 °C for 30 min. The mixture was poured into water (100 mL) and extracted with dichloromethane. The extract was successively washed with water, 5% sodium hydrogen carbonate aqueous solution, and brine. After the solvent had been evaporated, the residue was purified with column chromatography and recrystallization in methanol to provide **2** as a yellow solid (0.64 g, 80%). ^{1}H NMR ($CDCl_3$, 400 MHz): δ (ppm) 6.87 (d, 2H), 7.14 (d, 2H). ^{13}C NMR ($CDCl_3$, 400 MHz): δ (ppm) 115.6, 133.0.

Poly(9,9′-dioctylfluorene-*alt*-biselenophene) (F8Se2). To a stirred mixture of 2,7-bis(4,4,5,5,-tetramethyl-1,3,2-dioxaborolan-2-yl)-9,9′-dioctylfluorene (0.96 g, 1.53 mmol), 5,5-dibromo-2,2-biselenophene (0.64 g, 1.53 mmol), tetrakis(triphenylphosphine)-palladium (0.018 g, 0.015 mmol), and Aliquat 336 (0.062 g, 0.15 mmol) in anhydrous toluene (10 mL) was added a 2 M aqueous sodium carbonate solution (3.60 mL). The solution was refluxed with vigorous stirring for 3 days under a nitrogen atmosphere. An excess amount of bromobenzene (0.024 g, 0.15 mmol), the end-capper, dissolved in 2 mL of anhydrous toluene was added, and stirring and heating were continued for 12 h. The reaction mixture was then poured into methanol. The precipitated material was collected by filtration. The polymer was purified with column chromatography and reprecipitation in methanol. The crude polymer was first extracted consecutively with acetone in a Soxhlet apparatus. The residual insoluble component was then extracted consecutively with dichloromethane with the same method. Finally, a red polymer was obtained, yielding 1.2 g (75%). ^{1}H NMR ($CDCl_3$, 400 MHz): δ (ppm) aromatic; 7.78−7.24 (6H), 7.24−6.73 (4H) aliphatic; 2.01 (b, 4H) 1.87−0.05 (b, 30H). Anal. Calcd for $(C_{39}H_{50}Se_2)_n$: C, 69.22; H, 7.45. Found: C, 68.24; H, 7.09.

Instruments. Differential scanning calorimetry (DSC) and thermogravimetric analysis (TGA) were performed under a nitrogen atmosphere at a heating rate of 10 °C/min with a Dupont 9900 analyzer. Cyclic voltammograms (CV) of the polymer films (dip-coated onto Pt wire) were recorded on an AUTOLAB/PGSTAT12 at room temperature in a solution of tetrabutylammonium tetrafluoroborate (n-Bu_4NBF_4) (0.1 M) in acetonitrile under nitrogen gas protection at a scan rate of 50 mV/s. UV−vis measurements were carried out on a Jasco V-530, and the photoluminescence (PL) spectrum of the polymer was obtained using a Spex Fluolog-3 spectrofluorometer. Polarized optical micrographs were obtained using a Nikon ME600 inspection microscope attached to a DXM1200F digital camera. The temperature was controlled by using a Mettler FP82HT hot stage with a FP90 control processor.

Scheme 1. Synthetic Route for F8Se2[a]

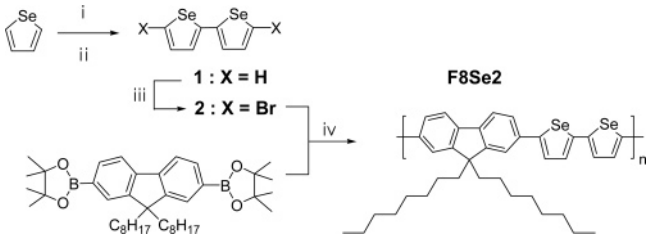

[a] Reagents and conditions: (i) n-BuLi, dry ether, 0 °C; (ii) $CuCl_2$, dry ether, −70 °C; (iii) NBS, $CHCl_3$: CH_3COOH (1:1), 50 °C; (iv) $Pd(PPh_3)_4$, Aliquat 336, aqueous Na_2CO_3, toluene, 80 °C.

XRD measurements were performed in the reflection mode at 30 kV and 60 mA with a scanning rate of 0.03° per 60 s and Cu Kα radiation (with wavelength λ = 1.5406 nm) using a Rigaku, D/max-rc (12 kW) generator.

Fabrication of the OFET Devices. Thin-film transistors were fabricated with a bottom contact geometry (channel width W = 100 μm, length L = 1 mm) with patterned AlNd gates and an insulating layer of poly(vinylphenol) (PVP) (dielectric constant = 4.2, $C_{ox} = 5.72 \times 10^{-9}$ F cm^{-2}). The spin-coated PVP film was cross-linked by heating at 100 °C for 10 min and again at 200 °C for 60 min. A 650 nm semiconductor layer of F8Se2 was deposited by spin-coating from a 0.5 wt % solution in chloroform. After spin-coating, the film was dried on a hot plate at 100 °C for 60 min in air or in a glovebox. All the electrical characteristics of the OTFT devices were measured in air. There was no difference between the performance of the devices prepared in air and those prepared in a glovebox.

Results and Discussion

Synthesis. Poly(9,9′-*n*-dioctylfluorene-*alt*-biselenophene) (F8Se2) was synthesized from the monomers 2,7-bis-(4,4,5,5,-tetramethyl-1,3,2-dioxaborolan-2-yl)-9,9′-dioctylfluorene[26] and 5,5′-dibromo-2,2′-biselenophene. The syntheses of the monomer containing selenophene and the resulting polymer are outlined in Scheme 1. The chemical structure of the polymer was verified with ^{1}H NMR, ^{13}C NMR, and elemental analysis. F8Se2 dissolves in common organic solvents such as chloroform and chlorobenzene without evidence of gel formation. The number-average molecular weight (M_n) of F8Se2, as determined with gel permeation chromatography (GPC) using a polystyrene standard, was found to be 72 600 (M_n/M_w = 1.6). The insoluble polymer present after the application of the acetone and dichloromethane extraction method to the crude polymer was found to have a narrow polydispersity coefficient and a well-defined molecular architecture.

Optical and Electrochemical Properties. Figure 1 shows the normalized UV−vis absorption and photoluminescence (PL) emission spectra of the polymer in the film state. The UV−vis absorption maximum and shoulder peaks appear at 517 and 486 nm, respectively, and the PL emission maximum appears at 578 nm with shoulder peaks at 540 and 623 nm. Both the absorption and emission peaks of F8Se2 are red-shifted by around 40−70 nm with respect to those of F8T2, a sulfur analogue of F8Se2.[26] The Se atom is larger and has stronger electron-donating abilities than the S atom, which may contribute to the observed red shift.[27,28]

The electrochemical behavior of the polymer was investigated using cyclic voltammetry (CV). The cyclic voltammogram of F8Se2 is shown in Figure 2. The onsets of oxidation and reduction were found to occur at 1.02 and −1.78 V (vs SCE), respectively, in the anodic and cathodic scans, which correspond to HOMO and LUMO levels of −5.41 and −2.61 eV, respectively, with respect to the energy level of the ferrocene

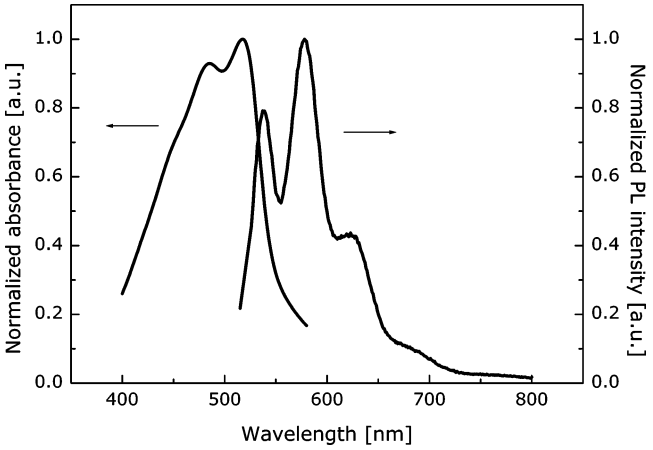

Figure 1. UV−vis absorption and PL emission spectra of a F8Se2 film.

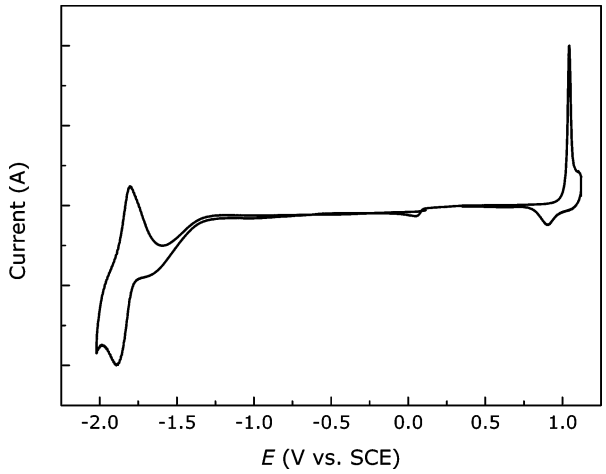

Figure 2. Cyclic voltammogram of F8Se2.

reference (−4.8 eV below the vacuum level).[29,30] The selenophene-based F8Se2 has a slightly higher HOMO energy level than the thiophene-based F8T2 (−5.5 eV).[31,32] The higher HOMO energy level of F8Se2 should result in improved hole injection in field effect transistors.

Liquid Crystalline Properties. Fluorene-based copolymers are known to exhibit liquid crystalline (LC) phases with high order parameters above their melting points. The phase transition temperatures of fluorene- and thiophene-based copolymers are more than 100 °C higher than that of the corresponding polyfluorene homopolymer due to the incorporation of rigid bithiophene or thieno[3,2-*b*]thiophene units.[21,33] Such phase transition behavior is also observed in F8Se2. The thermally induced phase transition behaviors of F8Se2 were investigated with differential scanning calorimetry (DSC). F8Se2 showed typical LC characteristics, i.e., both exothermal crystalline and endothermal liquid crystalline peaks. The crystallization and melting peaks of F8Se2 appear at 192 and 266 °C, respectively, as shown in Figure 3. The enthalpic changes of crystallization and melting are −6.38 and 2.96 J/g, respectively. In addition, F8Se2 was found to exhibit very good thermal stability, losing less than 5% of its weight on heating to about 420 °C, as determined with TGA under a nitrogen atmosphere (see the inset in Figure 3).

The thermotropic liquid crystalline properties of F8Se2 were also directly observed with polarized light microscopy (PLM). A film of the polymer was prepared on a quartz glass substrate by solution casting a solution of the polymer (1.0 wt %) in

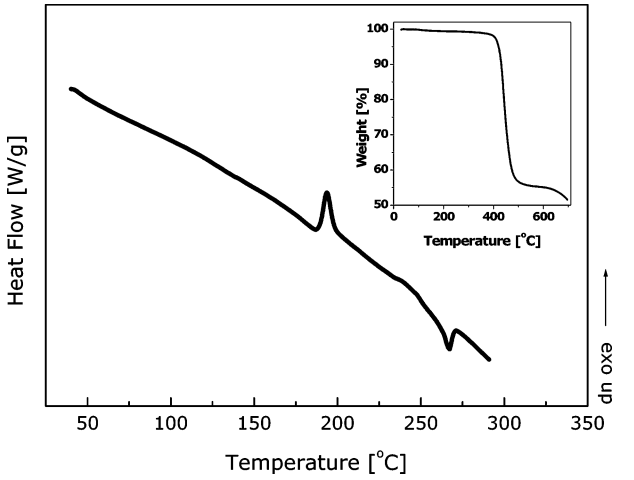

Figure 3. DSC thermogram of F8Se2 (inset: TGA curve of F8Se2).

chloroform. The film was then annealed to a temperature above the liquid crystalline transition and then quickly cooled to preserve liquid crystalline order.[34] The cast pristine film of the polymer did not exhibit birefringence due to its amorphous phase, whereas the film annealed to 270 °C produced a clear birefringent image due to the liquid crystalline domains, which is consistent with the phase transition characteristics revealed by the DSC analysis. Moreover, the film maintained its birefringence image after quick cooling to room temperature, as shown in Figure 4a. Figure 4b shows the corresponding PLM image recorded with the polarization direction of the light rotated by 90°. This difference in transmissivity shows that the domains are oriented to some degree in a liquid crystalline state. The thermotropic phase transition behavior of the polymer can result in the formation of highly ordered, closely packed structures, which could lead to an increase in charge carrier mobility within the domain boundaries.

The crystallization of F8Se2 was further confirmed by carrying out film and powder X-ray diffraction studies. Figure 5 shows the XRD patterns of a film cast onto a quartz glass substrate and of a powdery sample. In the XRD pattern of the film, there is a clear peak at 15.5 Å, which corresponds to the distance between the F8Se2 main chains separated by the octyl groups.[21] In the XRD pattern of the powder sample, a broad peak was observed at 4.8 Å, corresponding to the distance between the $\pi-\pi$ stacked molecular chains, along with a weak peak corresponding to the distance between the octyl side chains. The intensity distributions of the reflections from the lamellar layer structure and $\pi-\pi$ interchain stacking in the film and powder are very different. The peak at 15.5 Å caused by the lamellar layer structure is much larger and sharper in the film XRD pattern than in the powder XRD pattern. Such differences between the XRD patterns of powdery and cast film samples of π-conjugated polymers have been used to conclude that the polymer is aligned on the substrate.[8] Thus, this result suggests that the F8Se2 chains are aligned to a significant extent and separated from each other by octyl groups that are oriented normal to the substrate. This alignment of the polymer chains is expected to enhance the performance of F8Se2-based FET devices.

FET Characteristics. The F8Se2 thin-film transistors were found to exhibit typical p-channel FET characteristics. Plots of the transfer curve [i.e., $I_D = f(V_G)$] at constant $V_D = -20$ V and the hole mobility vs gate-source voltage characteristics of the F8Se2 device are shown in Figures 6 and 7, respectively. The field-effect mobility was calculated in the saturation regime

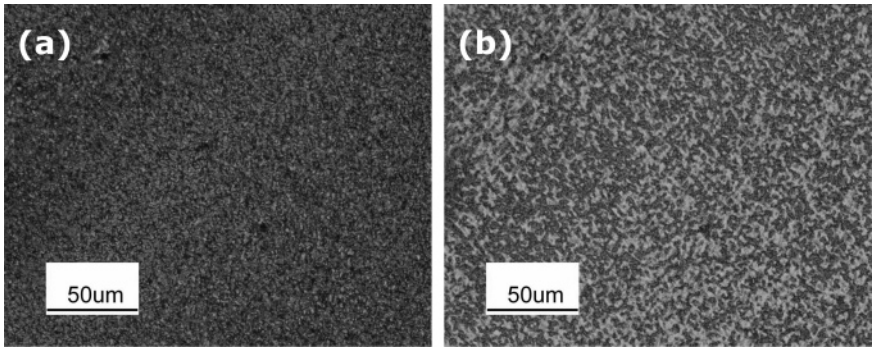

Figure 4. (a) PLM image of a quickly cooled F8Se2 film after annealing. (b) PLM image of the same sample but with the polarization direction of the light rotated by 90°.

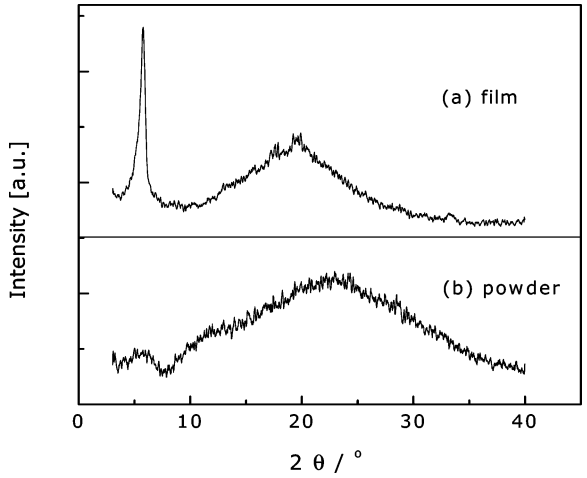

Figure 5. XRD patterns of F8Se2 as (a) a film and (b) a powder.

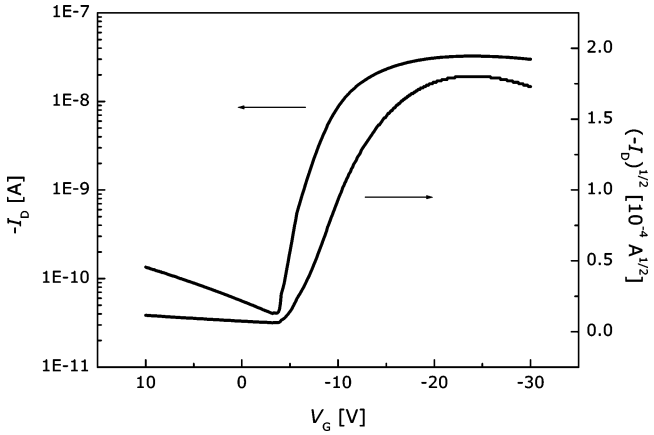

Figure 6. Transfer characteristics for the F8Se2 device(semilogarithmic plot of $-I_D$ vs V_G (left axis) and plot of $(-I_D)^{1/2}$ vs V_G (right axis)).

using the following equation:[35] $I_D = (W/2L)\mu C_i(V_G - V_T)^2$, where I_D is the drain-source current in the saturated region, W and L are the channel width and length, respectively, μ is the field-effect mobility, C_i is the capacitance per unit area of the insulation layer, and V_G and V_T are the gate and threshold voltages, respectively. The F8Se2 device switches on at a gate voltage of around -4 V, and its field effect mobility was found to be 0.012 $cm^2/(V\ s)$ at a gate voltage of around -8.4 V. This mobility was obtained without the use of any alignment technique and is reasonably high compared to those of other solution-processable π-conjugated polymers.[36] Selenophene is larger and has stronger electron-donating properties than thiophene, which result in increased electron density and π-conjugating electronic overlap between the polymer molecules. Further, as shown in the PLM and XRD results, the highly ordered structure of F8Se2 can play an important role in high carrier mobility. We conclude that the high mobility of F8Se2 results from the close molecular packing and well-defined orientation of the Se-containing polymer chains.

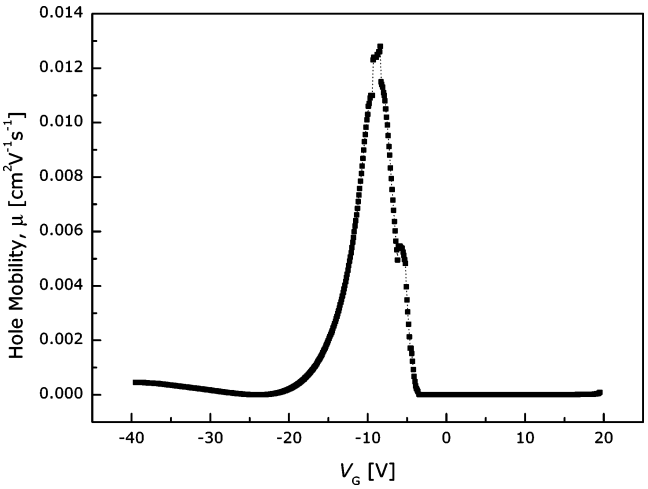

Figure 7. Hole mobility vs gate-source voltage characteristics of the F8Se2 device.

Conclusion

We have successfully synthesized a new conjugated copolymer based on fluorene and biselenophene, poly(9,9'-*n*-dioctylfluorene-*alt*-biselenophene) (F8Se2), via a palladium-catalyzed Suzuki coupling reaction. The thermotropic liquid crystallinity and chain alignment behavior of F8Se2 were demonstrated with DSC, PLM, and XRD analysis. The F8Se2 organic field effect transistor fabricated with a bottom contact geometry was found to exhibit a field effect mobility of 0.012 $cm^2/(V\ s)$. Our Se-containing copolymer, F8Se2, exhibits improved charge carrier mobility with respect to that of its sulfur analogue due to the electron-donating properties of selenium and the resulting stronger chain interactions between neighboring chains. We conclude that π-conjugated polymers containing selenophene are promising candidates for use in field effect transistors as active layers; the present results provide useful guidelines for the molecular design of high-mobility conjugated polymers for solution-processable OFET applications.

Acknowledgment. This work was supported by the Information Display R&D Center (No. AOD-02-A) through 21st Century Frontier R&D Program of Ministry of Science and Technology (MOST) and BK21. We gratefully acknowledge Mr. J. H. Kim and Prof. S. Y. Kim (KAIST) for the polarized light microscopy images.

References and Notes

(1) Burroughes, J. H.; Bradley, D. D. C.; Brown, A. R.; Marks, R. N.; Mackey, K.; Friend, R. H.; Burns, P. L.; Holmes, A. B. *Nature (London)* **1990**, *347*, 539−541.
(2) Friend, R. H.; Gymer, R. W.; Holmes, A. B.; Burroughes, J. H.; Marks, R. N.; Taliani, C.; Bradley, D. D. C.; Dos Santos, D. A.; Brédas, J. L.; Lögdlund, M.; Salaneck, W. R. *Nature (London)* **1999**, *397*, 121−128.
(3) Shim, H.-K.; Jin, J.-I. *Adv. Polym. Sci.* **2002**, *158*, 193−243.
(4) Katz, H. E.; Bao, Z.; Gilat, S. L. *Acc. Chem. Res.* **2001**, *34*, 359−369.
(5) Horowitz, G. *Adv. Mater.* **1998**, *10*, 365−377.
(6) Meng, H.; Bao, Z.; Lovinger, A. J.; Wang, B.-C.; Mujsce, A. M. *J. Am. Chem. Soc.* **2001**, *123*, 9214−9215.
(7) Babel, A.; Jenekhe, S. A. *Macromolecules* **2003**, *36*, 7759−7764.
(8) Yamamoto, T.; Kokubo, H.; Kobashi, M.; Sakai, Y. *Chem. Mater.* **2004**, *16*, 4616−4618.
(9) Schmidt-Mende, L.; Fechtenkötter, A.; Müllen, K.; Moons, E.; Friend, R. H.; MacKenzie, J. D. *Science* **2001**, *293*, 1119−1122.
(10) Brabec, C. J.; Sariciftci, N. S.; Hummelen, J. C. *Adv. Funct. Mater.* **2001**, *11*, 15−26.
(11) Cho, N. S.; Park, J. H.; Lee, J.; Lee, S. K.; Shim, H. K.; Park, M. J.; Hwang, D. H.; Jung, B. J. *Macromolecules* **2006**, *39*, 177−183.
(12) Lee, J.; Jung, B. J.; Lee, S. K.; Lee, J. I.; Cho, H. J.; Shim, H. K. *J. Polym. Sci., Part A* **2005**, *43*, 1845−1857.
(13) Crone, B.; Dodabalapur, A.; Lin, Y.-Y.; Filas, R. W.; Bao, Z.; LaDuca, A.; Sarpeshkar, R.; Katz, H. E.; Li, W. *Nature (London)* **2000**, *403*, 521−523.
(14) Gelinck, G. H.; Geuns, T. C. T.; de Leeuw, D. M. *Appl. Phys. Lett.* **2000**, *77*, 1487−1489.
(15) Klauk, H.; Jackson, N. *Solid State Technol.* **2000**, *43*, 63.
(16) Huitema, H. E. A.; Gelinck, G. H.; van der Putten, J. B. P. H.; Kuijk, K. E.; Hart, C. M.; Cantatore, E.; Herwig, T.; van Breemen, A. J. J. M.; de Leeuw, D. M. *Nature (London)* **2001**, *414*, 599.
(17) Lin, Y.-Y.; Gundlach, D. J.; Nelson, S. F.; Jackson, T. N. *IEEE Trans. Electron Devices* **1997**, *44*, 1325−1331.
(18) Cicoira, F.; Santato, C.; Dinelli, F.; Muria, M.; Loi, M. A.; Biscarini, F.; Zamboni, R.; Heremans, P.; Muccini, M. *Adv. Funct. Mater.* **2005**, *15*, 375−380.
(19) Bernius, M. T.; Inbasekaran, M.; O'Brien, J.; Wu, P. *Adv. Mater.* **2000**, *12*, 1737−1750.
(20) Sirringhaus, H.; Wilson, R. J.; Friend, R. H.; Inbasekaran, M.; Wu, W.; Woo, E. P.; Grell, M.; Bradly, D. D. C. *Appl. Phys. Lett.* **2000**, *77*, 406−408.
(21) Lim, E.; Jung, B.-J.; Lee, J.; Shim, H.-K.; Lee, J.-I.; Yang, Y. S.; Do. L.-M. *Macromolecules* **2005**, *38*, 4531−4535.
(22) Magdesieva, N. M.; Zefirovm, N. S. In *Organic Selenium Compounds; Their Chemistry and Biology*; Klayman, D. L., Gunther, W. H. H., Eds.; John Wiley: New York, 1973; p 425.
(23) Kunugi, Y.; Takimiya, K.; Toyoshima, Y.; Yamashita, K.; Aso, Y.; Otsubo, T. *J. Mater. Chem.* **2004**, *14*, 1367−1369.
(24) Takimiya, K.; Kunugi, Y.; Konda, Y.; Niihara, N.; Otsubo, T. *J. Am. Chem. Soc.* **2004**, *126*, 5084−5085.
(25) Kunugi, Y.; Takimiya, K.; Yamane, K.; Yamashita, K.; Aso, Y.; Ostubo, T. *Chem. Mater.* **2003**, *15*, 6−7.
(26) Lim, E.; Jung, B.-J.; Shim, H.-K. *Macromolecules* **2003**, *36*, 4288−4293.
(27) Yang, R.; Tian, R.; Hou, Q.; Yang, W.; Cao, Y. *Macromolecules* **2003**, *36*, 7453−7460.
(28) Crouch, D. J.; Skabara, P. J.; Lohr, J. E.; McDouall, J. J. W.; Heeney, M.; McCulloch, I.; Sparrowe, D.; Shkunov, M.; Coles, S. J.; Horton, P. N.; Hurshouse, M. B. *Chem. Mater.* **2005**, *17*, 6567−6578.
(29) Pommerehe, J.; Vestweber, H.; Guss, W.; Mahrt, R.; Bassler, H. F.; Porsch, M.; Daub, J. *Adv. Mater.* **1995**, *7*, 551−554.
(30) Meng, H.; Zheng, J.; Lovinger, A. J.; Wang, B.-C.; Patten, P. G. V.; Bao, Z. *Chem. Mater.* **2003**, *15*, 1778−1787.
(31) Beaupré, S.; Blondin, P.; Ranger, M.; Bouchard, J.; Leclerc, M. *Chem. Mater.* **2000**, *12*, 1931−1936.
(32) Stutzmann, N.; Friend, R. H.; Sirringhaus, H. *Science* **2003**, *299*, 1881−1884.
(33) Kawana, S.; Durrell, M.; Lu, J.; Macdonald, J. E.; Grell, M.; Bradley, D. D. C.; Jukes, C.; Jones, R. A. L.; Bennett, S. L. *Polymer* **2002**, *43*, 1907−1913.
(34) Grell, M.; Bradly. D. D. C.; Inbasekaran, M.; Woo, E. P. *Adv. Mater.* **1997**, *9*, 798−802.
(35) Dimitrakoupoulos, C. D.; Melenfant, P. R. L. *Adv. Mater.* **2002**, *14*, 99−117.
(36) Sirringhaus, H. *Adv. Mater.* **2005**, *17*, 2411−2425.

MA060567L